Available online at www.sciencedirect.com

ScienceDirect

Transportation Research Procedia 2 (2014) 149 – 158

Transportation Research Procedia

www.elsevier.com/locate/procedia

The Conference on Pedestrian and Evacuation Dynamics 2014 (PED2014)

Pedestrian group behaviour analysis under different density conditions

Francesco Zanlungo [a,*], Dražen Brščić [a], Takayuki Kanda [a]

[a] *IRC-ATR, Kyoto, Japan and JST CREST Tokyo, Japan*

Abstract

We recently introduced a potential to describe pedestrian interaction in walking groups. The potential was used to derive the spatial distribution and velocity of small groups under scarce density conditions and its predictions are in good agreement with observations. In the present work we apply the same method to a new data set regarding pedestrians moving in an indoor facility under different density conditions. To describe the variation of the group structure with changing density we introduce an "effective potential" term that assesses the average effect of the external environment on the group dynamics.

© 2014 The Authors. Published by Elsevier B.V. This is an open access article under the CC BY-NC-ND license (http://creativecommons.org/licenses/by-nc-nd/3.0/).

Peer-review under responsibility of Department of Transport & Planning Faculty of Civil Engineering and Geosciences Delft University of Technology

Keywords: group behaviour

1. Introduction

Social groups represent an important component of urban crowds, reaching in some environments up to 85% of the walking population Schultz et al. (2014); Moussaïd et al. (2010), but until recent times their effects have been largely ignored in the development of microscopic crowd dynamics models. Nevertheless, it has to be expected that such groups, walking in a characteristic configuration (Schultz et al. (2014); Moussaïd et al. (2010); Costa (2010); Zanlungo and Kanda (2013)) and with slower velocity (Zanlungo et al. (2014)), have an important influence on the dynamics of the crowd. In the last years a few models describing group dynamics have been developed (Moussaïd et al. (2010); Köster et al. (2011); Karamouzas and Overmars (2010); Zhang et al. (2011)). In Zanlungo et al. (2014) we developed a mathematical model for the spatial dynamics of socially interacting pedestrians. The model is based on a non Newtonian potential and describes qualitatively the spatial structure and velocity of 2 people groups; furthermore, once calibrated on 2 people groups, it describes the shape and velocity of larger groups. Nevertheless, the model has been developed under the assumption that social interaction is the leading dynamics term, i.e., that pedestrians are walking in a wide and low density environment. In this work we investigate the validity of our approach at higher densities.

* Corresponding author. Tel.: +0-000-000-0000 ; fax: +0-000-000-0000.
E-mail address: author@institute.xxx

2352-1465 © 2014 The Authors. Published by Elsevier B.V. This is an open access article under the CC BY-NC-ND license (http://creativecommons.org/licenses/by-nc-nd/3.0/).
Peer-review under responsibility of Department of Transport & Planning Faculty of Civil Engineering and Geosciences Delft University of Technology
doi:10.1016/j.trpro.2014.09.020

2. Potential for group interaction

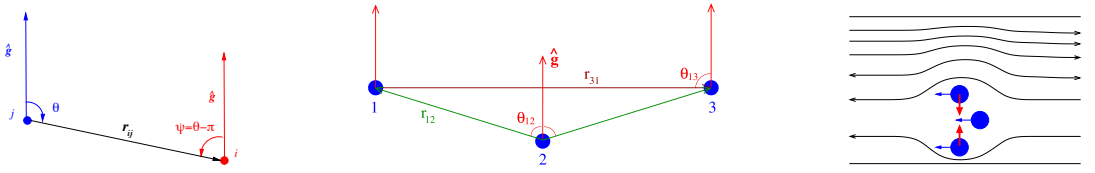

(a) (b) (c)

Fig. 1: (a): r and θ give the position of pedestrian i with respect to j. $|\theta|$ is the angle that j's gaze has to span between the goal direction $\hat{\mathbf{g}}$ and i, while the corresponding angle for i is given by $|\psi|$. (b): equilibrium configuration for a group of 3, and definition of the variables r_{12}, θ_{12}, r_{13} and θ_{13}. For $\eta < 0$ we have a "V" formation with $|\theta_{12}| < \pi/2$. (c): if a social group is perceived as a unit by others, and interactions happen mainly on its borders, the average effect of the environment may be expressed as a force toward the centre of the group and orthogonal to the corridor axis.

2.1. Mathematical formulation

Let us assume, following Zanlungo et al. (2014), to which the reader should refer for further details, that 2 pedestrians, identified as i and j, are socially interacting while walking towards a common goal, given by a versor $\hat{\mathbf{g}}$. Their relative position, $\mathbf{r} \equiv \mathbf{r}_{ij} \equiv \mathbf{r}_i - \mathbf{r}_j$, may be written in polar coordinates as (r, θ), where $-\pi < \theta \leq \pi$ is the angle between $\mathbf{r}_{ij}$ and $\hat{\mathbf{g}}$ (see Fig. 1a). Defining

$$\psi \equiv \begin{cases} \theta - \pi \text{ if } \theta > 0, \\ \theta + \pi \text{ if } \theta \leq 0, \end{cases} \tag{1}$$

we see that $|\psi|$ is the angle that i's gaze has to span between the goal and the interaction partner, while $|\theta|$ is the corresponding angle for j. We expect pedestrians to want the goal in their vision field; furthermore, for social interaction they want also their partner in their vision field (Knapp (2012)), but they also want to be in the partner's vision field, so that their gazes may meet (Kleinke (1986)). We may thus suppose that i feels a *discomfort*, i.e. a difficulty in *walking towards* $\hat{\mathbf{g}}$ *while socially interacting with* j, that grows with $|\theta|$ and $|\psi|$. Let us assume such a discomfort to be quadratic[1] as

$$\Theta^\eta(\theta) = (1+\eta)\theta^2 + (1-\eta)\psi^2, \qquad -1 \leq \eta \leq 1. \tag{2}$$

We expect discomfort to have also a radial component, since there will be a distance r_0 at which social interaction is maximally comfortable Yücel et al. (2013). We can ask this potential to diverge for $r \to 0$ to avoid physical overlapping, and to grow linearly for $r \to \infty$ so that two interacting pedestrians are a bounded system and the interaction force saturates to a constant value. We may pose[2]

$$R(r) = \frac{r}{r_0} + \frac{r_0}{r}. \tag{3}$$

Let us assume r and θ to be independent and define the *potential discomfort of* i *when interacting with* j

$$U^\eta_{ij}(r, \theta) = C_r R(r) + C_\theta \Theta^\eta(\theta). \tag{4}$$

Assuming that pedestrian i tries to minimise such a function, we may postulate its actions to determinate

$$\dot{\mathbf{v}}_i = \mathbf{F}_{ij} = -\nabla_i U^\eta_{ij}(\mathbf{r}_i - \mathbf{r}_j). \tag{5}$$

[1] Since any smooth potential is quadratic close to equilibrium (Landau and Lifshitz (1976)), this choice is natural in absence of further evidence.
[2] We chose this formula for simplicity's sake; it describes well pedestrian interactions close to the potential minima, but it fails very far from the minima, probably due to the fact that when pedestrians get far from each other they stop interacting.

In Cartesian coordinates[3] we have

$$F_x^\eta = \frac{C_r}{r_0}\left(\frac{r_0^2}{r^2}-1\right)\sin\theta - \frac{4}{r}C_\theta(\theta-\theta_{\mathrm{sgn}(\theta)})\cos\theta, \qquad F_y^\eta = \frac{C_r}{r_0}\left(\frac{r_0^2}{r^2}-1\right)\cos\theta + \frac{4}{r}C_\theta(\theta-\theta_{\mathrm{sgn}(\theta)})\sin\theta, \tag{6}$$

where $\theta_\pm$ are the angles at which the angular potential attains a minimum,

$$\theta_\pm = \pm(1-\eta)\frac{\pi}{2}. \tag{7}$$

Let us stress that that $U_{ij}^\eta(\mathbf{r}_i - \mathbf{r}_j)$ is not the potential of the (i, j) system, but only of the pedestrian i; if $\eta \neq 0$ we have $U^\eta(-\mathbf{r}) \neq U^\eta(\mathbf{r})$, and thus $U_{ij}^\eta \neq U_{ji}^\eta$, from which $\mathbf{F}_{ij} \neq -\mathbf{F}_{ji}$ follows, and thus the system does not satisfy Newton's third law and conservation of momentum Landau and Lifshitz (1976). Indeed we have for the centre of mass of the (i, j) system[4]

$$\dot{V}_x^\eta = -\eta\frac{2\pi}{r}C_\theta\cos\theta, \qquad \dot{V}_y^\eta = \eta\frac{2\pi}{r}C_\theta\sin\theta. \tag{8}$$

On the opposite, we may show that the relative dynamics is given by a Newtonian potential

$$\dot{\mathbf{v}} \equiv \ddot{\mathbf{r}}_i - \ddot{\mathbf{r}}_j = -2\nabla U^0(\mathbf{r}). \tag{9}$$

This potential describes pedestrian behaviour close to potential minima (optimal interaction positions); assuming the environment to be wide enough and at low enough density we may expect a group of 2 pedestrians to be close to such a configuration, and approximate the interaction with the environment with a white noise term $\boldsymbol{\Xi}$ (with standard deviation σ). Following Helbing and Molnar (1995), we assume the influence of the common goal to be given by the drag[5]

$$\mathbf{F}_i^g = \kappa(\mathbf{v}_p - \mathbf{v}_i), \qquad \mathbf{v}_p = v^{(1)}\hat{\mathbf{g}}. \tag{10}$$

As a result the dynamics of the centre of mass for a 2 people group is[6]

$$\dot{\mathbf{V}} = \kappa(\mathbf{v}_p - \mathbf{V}) + \dot{\mathbf{V}}^\eta, \tag{11}$$

while the relative dynamics is given by the stochastic equation

$$\dot{\mathbf{v}} = -\kappa\mathbf{v} - 2\nabla U^0(\mathbf{r}) + \boldsymbol{\Xi}. \tag{12}$$

We may then assume that the probability distribution function for the equilibrium distribution of the relative distance between pedestrians in a group of 2 is given by the Boltzmann canonical distribution of statistical mechanics[7] Landau and Lifshitz (1980),

$$\rho(\mathbf{r}) \propto \exp(-\beta U^0(\mathbf{r})). \tag{13}$$

2.2. Interpretation and consequences

The relative dynamics of a group of two pedestrians is determined by eq. (9), in which η does not appear, and its equilibrium configuration is an abreast one. Nevertheless, the group as a whole feels the effect of the non Newtonian term eq. (8), which for an abreast configuration is aligned with the goal direction, in particular opposite to it for $\eta < 0$.

[3] Assuming the y axis to be aligned with $\hat{\mathbf{g}}$.
[4] Here we assume $0 < \theta \leq \pi$ to be the angle giving the position of the pedestrian on the right.
[5] We use $\kappa = 1.52\ \mathrm{s}^{-1}$, see Zanlungo et al. (2011). $v^{(1)}$ is the individual pedestrian preferred velocity.
[6] Recalling eq. (8) and ignoring stochastic terms.
[7] We are assuming an ergodic point of view, and considering the distribution after integration over time and different groups as equivalent to the equilibrium one, refer to Zanlungo et al. (2014) for details.

Recalling eq. (2), $\eta < 0$ corresponds to giving a higher discomfort value to the angle that one's gaze has to span between the goal and the partner position, with respect to the angle that the partner's gaze has to span. As a result the abreast configuration is not comfortable and the pedestrian is slowed down by a factor (*load of interaction*)

$$\Delta v^{(2)} \equiv v^{(2)} - v^{(1)} = \eta C_\theta \frac{2\pi}{r\kappa} \equiv \frac{\Delta a^{(2)}}{\kappa}, \tag{14}$$

where $v^{(1)}$ is the preferred velocity of single pedestrians, and $v^{(2)}$ the velocity of groups of 2.

We assume that in larger groups the effect of the potential (4) is non negligible only for first neighbours; as a result for an abreast group of 3 people, the central pedestrian is slowed down by a factor $2\Delta a^{(2)}$, compared to the factor $\Delta a^{(2)}$ of the pedestrians on the wings. The equilibrium configuration is thus a V formation (Fig. 1b)[8], and the velocity can be fairly well approximated taking in consideration the total force $4\Delta a^{(2)}$ felt in the abreast configuration[9], i.e.

$$\Delta v^{(3)} \equiv v^{(3)} - v^{(1)} \approx \frac{4}{3} \eta C_\theta \frac{2\pi}{r\kappa} = \frac{4}{3} \Delta v^{(2)}. \tag{15}$$

2.3. Calibration and validation

We compared these predictions with the behaviour of actual pedestrians, tracked using 2D laser range sensors (Glas et al. (2009)) in a pedestrian facility in the underground Umeda (central Osaka) area whose main corridors were large $\approx 6 - 7$ m and with a ≈ 0.03 ped/m^2 density[10]. The area was also video recorded, and two different "coders" analysed the images to provide the social interaction ground truth[11]. Fig. 2a shows a comparison between the empirical distribution of pedestrian relative position for a group of 2 with the calibrated distribution given by eq. (13)[12]. Fig. 2b shows the evaluation of the model on 3 people groups, i.e. a comparison between the empirical 3 people distribution and the one predicted by the model. The values of the main 2 and 3 people observables in the Umeda set are reported in Table 4; giving $v^{(1)}$ and $v^{(2)}$ as an input to the 3 people model, we obtained $v^{(3)} = 1098$ mm/s, in good agreement with the observed value. After checking the ability of the model to reproduce the 3 people group behaviour, we calibrated the model on 2 and 3 people behaviour, obtaining parameters shown in Table 3 and observable values shown in Table 4.

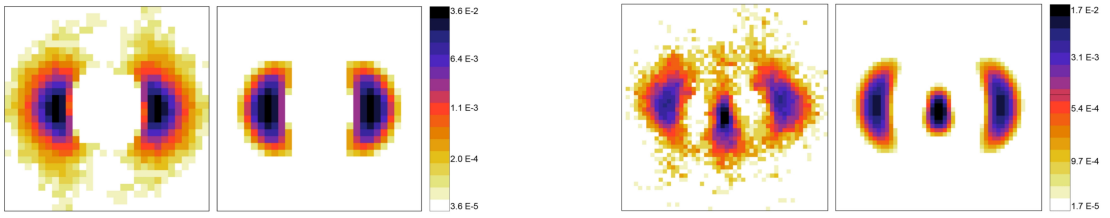

(a) (b)

Fig. 2: (a): empirical 2 people relative distance distribution compared to the best fit of eq. (13). (b): empirical 3 people distribution (in the centre of mass frame) compared to the prediction of the model calibrated in (a).

3. A new data set

To investigate how social group behaviour changes at higher densities, we collected data in a different environment. As explained in detail in Brščić et al. (2013), we collected more than 800 hours of pedestrian data using a system of

[8] Assuming $\eta < 0$. For $\eta > 0$ we would have an accelerated Λ formation, and obviously a normal speed abreast formation for $\eta = 0$.

[9] The exact result involves a numerical solution, see Zanlungo et al. (2014) for details.

[10] We assume our model for a group of n pedestrians to be valid in corridors wider than nr_0 and the density lower than $(nr_0)^{-2}$ (Zanlungo et al. (2014)).

[11] While tracking was performed also in some 4 m wide corridors, video recording was limited to the main corridors.

[12] By calibrated we mean the distribution given using the parameters β, r_0, C_θ and η that better fit the empirical 2 people distribution.

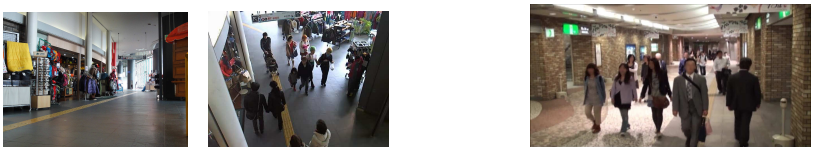

(a) (b)

Fig. 3: (a): ATC environment. (b) Umeda environment.

3D laser range sensors (Brščić et al. (2013)) in a 900 m^2 area of the ATC centre in Osaka. This environment includes a corridor (shown in Fig. 3 compared to the environment analysed in Zanlungo et al. (2014)) connecting two different busy areas. We analysed group behaviour in an area of this corridor a with a 12 m length and 3.5 m width in which pedestrian density is almost invariant along the corridor's main axis[13], and dropping to zero at the corridor's border[14]; nevertheless, as shown in the figure, the environment studied in this work is qualitatively different from the one studied in Zanlungo et al. (2014) by not having well defined borders limited by walls. For this work the analysis of social interactions was performed by one of the coders we used in Zanlungo et al. (2014) on 1% of available data (Table 1). The coder identified a number of socially interacting groups comparable to that of Zanlungo et al. (2014). Nevertheless, due to the limited size of the environment, the number of data points was considerably reduced. For this reason, in order to have a significant amount of data for each density condition, we divide our data in two sets, *high density* with $\rho \geq 0.098$ ped/m^2 and *low density* with $\rho \leq 0.06$ [15]. The average velocities of groups and individuals are shown in Table 4. Figs. 4-5 show the probability distributions for the 2 and 3 people observables defined in Fig. 1. The averages, variations and modes of these observables are in Table 4[16].

Table 1: Pedestrian densities (ped/m^2) in the ATC data set, for different dates and time (*high density* in boldface).

	10-11	12-13	15-16	19-20
2013/01/09 (Wed)	0.017	0.06	0.031	0.016
2013/02/17 (Sun)	0.046	**0.098**	**0.099**	0.024

3.1. Qualitative analysis

In eq. (12), the effect of the external environment (including walls and other pedestrians) is given by the stochastic term $\boldsymbol{\Xi}$. With increasing density, the standard deviation σ of $\boldsymbol{\Xi}$ is expected to grow, along with the system's "temperature" $1/\beta$. As a result (eq. 13) the spread of the distributions in figures 4-5 should increase. Nevertheless, *if the assumptions that lead us to eq. (12) are valid*, the position of the maxima of these distributions should not change. One of these assumptions was that $\boldsymbol{\Xi}$ is a white noise, i.e. that the effect of the environment had no preferential direction on the group dynamics. This assumption is not valid when the size of the corridor gets comparable to the size

[13] Knowing with a good precision the pedestrian density at which the social interaction happens is of obvious relevance to the scope of this work.
[14] Refer to Brščić et al. (submitted) for details; consistently with Zanlungo et al. (2014) we analysed only *moving* pedestrians with $v > 0.5$ m/s, also when measuring density.
[15] We also tried a *medium density* set with $0.046 \leq \rho \leq 0.06$, but the results were qualitatively equivalent to those of *low density*.
[16] For θ_{13} (Fig. 5c), no clear peak is present. While for *high density* the average value of $|\theta_{12}|$ increases with respect to *low density*, this is due to the fact that the V formation is so accentuated in *high density* that we have switches in position between the central and the wing pedestrians. For distributions with such a wide spread a description based on angular statistics would be probably more effective. We also notice that, in both environments the distributions of θ for 2 people and θ_{13} for 3 people are very similar.

Table 2: Socially interacting groups detected in each data set (and corresponding number of data points).

	Umeda	ATC	*low density*	*high density*
2 people	854 (70513)	951 (17141)	404 (7131)	547 (10028)
3 people	102 (8721)	189 (2778)	83 (1085)	106 (1693)

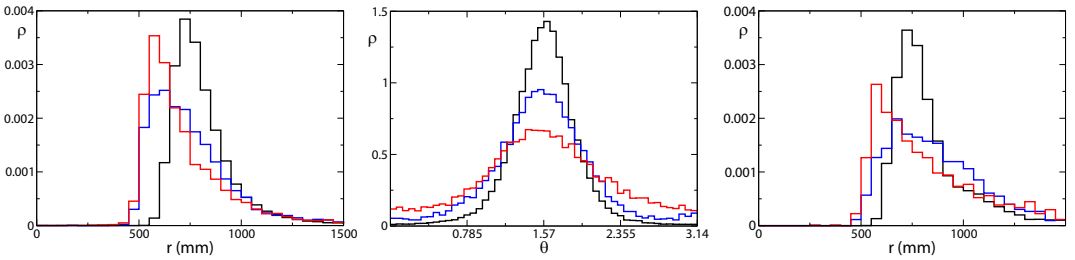

(a) (b) (c)

Fig. 4: (a): comparison between the 2 people r distribution in the Umeda (black), *low density* (blue) and *high density* (red) sets. (b): same comparison for θ. (c): same comparison for the 3 people r_{12} distribution.

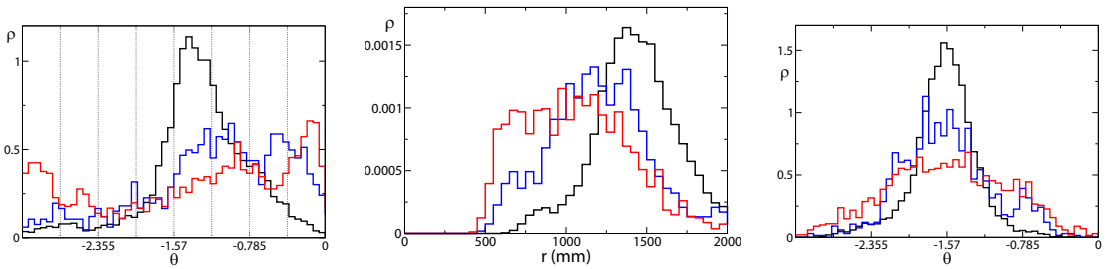

(a) (b) (c)

Fig. 5: (a): comparison between the 3 people θ_{12} distribution in the Umeda (black), *low density* (blue) and *high density* (red) sets. (b): same comparison for r_{13}. (c): same comparison for θ_{13}.

of the group, since the "pressure" from the environment should be mainly directed towards the centre of mass of the group. Supposing that the surrounding pedestrians treat a group as a unit, and thus that collision avoiding interactions happen mainly at the borders of the group, we may expect also high pedestrian densities to have a similar effect. Furthermore, since Japanese pedestrians walk preferentially on the left side (Brščić et al. (submitted); Zanlungo et al. (2012)), the corridor has, from the point of view of the space available to the group, an "effective" width, equal to half of the actual width (see Fig. 1c).

The flow of pedestrians in the ATC corridor is distributed on a width of 3.5 m, and thus its "effective" width is 1.75 m, comparable to the size of 2 and 3 people groups. Indeed pedestrian distributions in ATC are different from those in Umeda, not only in their larger spreads but also in the position of the maxima, including in the *low density* set whose pedestrian density is comparable to the Umeda one. Pedestrians are closer between them in ATC than in Umeda, and

closer at *high density* than at *low density*. Furthermore in ATC the V formation is more "closed" (smaller values of $|\theta_{12}|$). Such observations seem in good qualitative agreement with the idea that the average effect of the environment is equivalent to a pressure towards the centre of the group.

Also in ATC we find a decrease in velocity with the growing size of groups, that for the *high density* set is in good agreement with eq. (15), while in the *low density* set the velocity of 3 people groups is slightly slower than expected. We should nevertheless stress that without a proper theory of the effect of the environment on the velocity of individuals and groups, we shouldn't necessarily expect eq. (15) to be valid outside the conditions under which we derived it[17].

4. An effective potential for the environmental effect

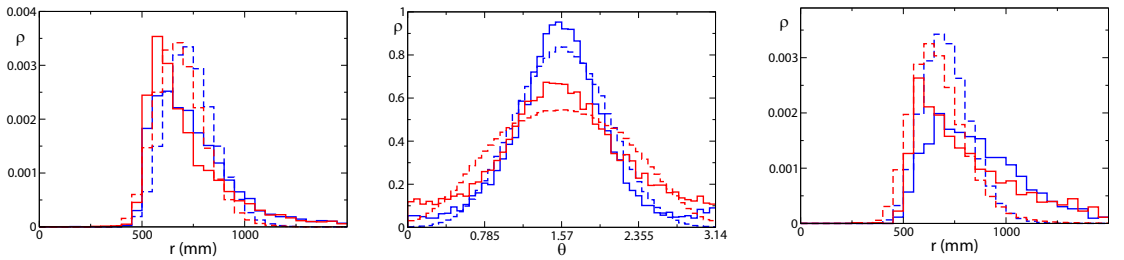

Fig. 6: (a): comparison between the 2 people empirical r distributions (continuous lines) with their calibrated versions coming from the effective potential eq. (16); *low density* in blue and *high density* in red. (b): same comparison for θ. (c): comparison between the 3 people empirical r_{12} distributions (continuous line) with those obtained by numerically integrating the 3 people version of the stochastic equation 12 using the effective potential of eq. (16) calibrated on the distributions of Fig. 6a-6b; *low density* in blue and *high density* in red.

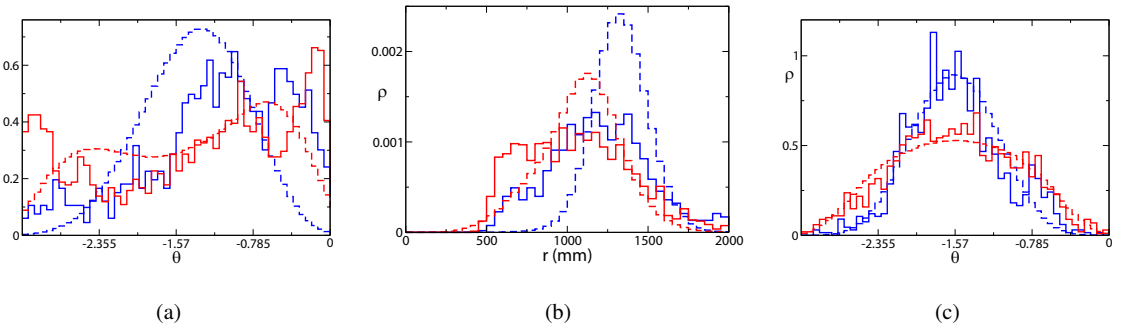

Fig. 7: (a): comparison between the 3 people empirical θ_{12} distributions (continuous line) with those obtained by numerically integrating the 3 people version of the stochastic equation 12 using the effective potential of eq. (16) calibrated on the distributions of Fig. 6a-6b; *low density* in blue and *high density* in red. (b): same comparison for r_{13}. (c): same comparison for θ_{13}.

[17] There are two possible problems related to the tracking method. First, the tracking sensors and algorithms used in Umeda and in ATC are different, and even if we are not aware of any effect that could lead to it, we cannot exclude the possibility of a systematic difference between them. Second, to improve tracking stability a limit of $\approx$ 500 mm is imposed on the distance between pedestrians. While the Umeda distributions were far from such a limit, the ATC ones get close to it, and as result it is difficult to understand if the very steep growth in the r distributions around such a limit corresponds to actual pedestrian behaviour or is a tracking algorithm artifact. This steep growth is very difficult to model using eq. (3).

We plan to reproduce the effect of the environment using a purely microscopic model based only on individual interactions. Nevertheless, for the extent of this work we develop a model in which the microscopic properties of the group are determined by a macroscopic parameter (pedestrian density) through the addition of an effective term to the potential. There are two reasons to attempt such a formulation. First of all, we get some theoretical insight about the average effect of the environment on group behaviour. Furthermore, using such a model we may reproduce the group position probability density distribution through eq. (13)[18], without having to rely on computationally expensive many agent simulations[19].

Following Fig. 1c we assume that the effect of the environment on the group centre of mass dynamics is given by a force directed towards the centre of the group and perpendicular to the corridor axis[20]. We expect this force to grow with the distance from the group's centre, and assume that the group dynamics in an environment with density ρ_{env}[21] is given by adding to U^0 (eq. 9) the term[22]

$$U_{\mathrm{eff}} = \frac{1}{2} C_{\rho_{\mathrm{env}}} \left(\frac{x}{r_0} \right)^2, \qquad x = r \sin\theta. \tag{16}$$

Let us assume the environment to have a "friction" effect on all pedestrians, individuals or in group (thus without effect on group dynamics) as[23]

$$-\lambda_{\rho_{\mathrm{env}}} \mathbf{v}. \tag{17}$$

We also assume η and obviously the standard deviation σ of Ξ to be functions of ρ_{env}[24], while we assume r_0, C_θ and C_r to be environment independent. Since parameters $C_{\rho_{\mathrm{env}}}$, η and σ may be calibrated on 2 people pedestrian distribution and velocities[25], the proposed effective model may be evaluated by comparing its predictions with the empirical 3 people group distributions.

The results of calibration on 2 people groups are shown in Table 3. We do not have enough data points to fully understand how these parameters change with density, but we may see that, as expected, σ and $C_{\rho_{\mathrm{env}}}$ grow with density, while $|\eta|$ goes down (social interaction decreases as we move to more dense environments).

5. Results

Figs. 6-7 compare for each set the empirical 2 people probability distributions with those obtained calibrating the model, and the empirical 3 people distributions with the model evaluation ones (observables defined in Fig. 1). Averages, standard deviations and maxima positions are given in Table 4. The effective model, despite its simplicity, describes fairly well the position of the maxima of all distributions. 3 people distributions are described better in the *high density* set than in the *low density* one[26]. Angular distributions are very well reproduced both in calibration and evaluation, with the partial exception of θ_{12}. For this distribution we have nevertheless the interesting prediction, for *high density*, of the splitting of the global maximum in two local maxima, a stronger one close to 0 and a weaker one close to $-\pi$, a prediction that seems to be in qualitative agreement with the data[27]. The "fat tails" of radial distributions result to be particularly difficult to describe in the high noise regime; this is not surprising considering that the model

[18] In case of larger groups, through a numerical integration of the multi-pedestrian version of eq. (12), see Zanlungo et al. (2014).

[19] The knowledge of density dependent distributions is necessary to extend to different environments the group recognition approach of Yücel et al. (2013).

[20] That we may consider to be aligned with the group goal direction $\hat{\mathbf{g}}$.

[21] Such a parameter should include also the effect of the corridor's width.

[22] We use r_0 to have $C_{\rho_{\mathrm{env}}}$ of the same dimensionality as C_r and C_θ.

[23] This term can be calibrated just comparing the velocity of single pedestrians in the set with the one in Umeda.

[24] Since η is connected to the slowing down of pedestrians due to social interaction, we expect such a a parameter to be modified in different conditions that may affect social interaction.

[25] We follow the same approach as in Zanlungo et al. (2014) and we calibrate $C_{\rho_{\mathrm{env}}}$ using eq. (13) and η, σ using numerically integrating eq. (12).

[26] Interestingly, if we replace $x = r\sin\theta$ with r in eq. (16), we get a better description for *low density* than for *high density*; the effect of the environment seems thus to be a "central potential" Landau and Lifshitz (1976) for low densities, and to become orthogonal to the corridor axis for higher densities. We stick to the orthogonal term since the high density regime is more interesting by being the one that diverges more from the original model.

[27] This happens because the effective term makes Λ formations metastable, a result that could not be attained with a radial term.

has been developed to describe the behaviour close to the potential minima, nevertheless a modification of eq. (3) (introducing a logarithmic growth for large r instead of a linear one) could be taken in consideration. We finally notice that the 3 people group velocity is quantitatively well described in the *high density* set; in the *low density* one the qualitative decrease of velocity is described, but we find a 40 mm/s difference between the empirical value and the prediction of our model, corresponding more or less to the sum of the $v^{(2)}$ and $v^{(3)}$ standard errors.

Table 3: Model parameters in different data sets. r_0 in meters, C_r, C_θ and $C_{\rho_{\rm env}}$ in square meters over seconds, σ in meters over seconds, $\lambda_{\rho_{\rm env}}$ in seconds^{-1}.

	r_0	C_r	C_θ	η	σ	$C_{\rho_{\rm env}}$	$\lambda_{\rho_{\rm env}}$
Umeda	0.745	0.62	0.08	-0.43	0.77	0	0
low density	0.745	0.62	0.08	-0.26	1.13	0.12	0.137
high density	0.745	0.62	0.08	-0.22	1.25	0.34	0.393

Table 4: Average values, standard deviations and maxima position (in brackets) of the main observables (as defined in Fig. 1) in the different data (empirical and simulations). Distances in meters, velocities in mm/s, angles in radians. Velocities are shown for empirical sets along with standard errors in place of standard deviations.

	r	θ	r_{12}	θ_{12}
Umeda	0.82 ± 0.19 (≈ 0.73)	1.57 ± 0.31 ($\approx \pi/2$)	0.85 ± 0.22 (≈ 0.73)	-1.29 ± 0.54 (≈ -1.42)
low density	0.78 ± 0.27 (≈ 0.63)	1.56 ± 0.51 ($\approx \pi/2$)	0.92 ± 0.35 (≈ 0.68)	-1.29 ± 0.54 (≈ -1.41)
high density	0.74 ± 0.26 (≈ 0.58)	1.58 ± 0.66 ($\approx \pi/2$)	0.85 ± 0.31 (≈ 0.58)	-1.11 ± 0.82 ($\approx -1.$)
Umeda model	0.77 ± 0.1 (≈ 0.77)	1.57 ± 0.29 ($\approx \pi/2$)	0.81 ± 0.1 (≈ 0.78)	-1.26 ± 1.1 (≈ -0.15)
low density model	0.74 ± 0.12 (≈ 0.73)	1.57 ± 0.44 ($\approx \pi/2$)	0.71 ± 0.12 (≈ 0.68)	-1.38 ± 0.52 (≈ -1.35)
high density model	0.69 ± 0.12 (≈ 0.68)	1.57 ± 0.59 ($\approx \pi/2$)	0.68 ± 0.14 (≈ 0.63)	-1.35 ± 0.95 ($\approx -2.4- \approx -0.7$)

	r_{13}	θ_{13}	$v^{(1)}$	$v^{(2)}$	$v^{(3)}$
Umeda	1.46 ± 0.31 (≈ 1.43)	-1.59 ± 0.32 ($\approx -\pi/2$)	1336 ± 2	1159 ± 6	1112 ± 17
low density	1.24 ± 0.37 (≈ 1.2)	-1.57 ± 0.47 ($\approx -\pi/2$)	1226 ± 5	1132 ± 11	1056 ± 25
high density	1.09 ± 0.39 (≈ 1.0)	-1.57 ± 0.64 ($\approx -\pi/2$)	1062 ± 4	999 ± 8	978 ± 18
Umeda model	1.57 ± 0.14 (≈ 1.55)	-1.57 ± 0.25 ($\approx -\pi/2$)	1336	1160	1110
low density model	1.33 ± 0.17 (≈ 1.33)	-1.57 ± 0.42 ($\approx -\pi/2$)	1226	1132	1097
high density model	1.08 ± 0.25 (≈ 1.13)	-1.57 ± 0.65 ($\approx -\pi/2$)	1062	998	986

6. Conclusions

We compared the prediction of our group behaviour model, developed for and tested in the low-density, wide environment regime, with the behaviour of pedestrians in a more narrow and dense environment. As expected, the pedestrian distributions resulted to be qualitatively different, nevertheless we showed that the qualitative behaviour of 2 and 3 people groups can be described at higher densities by introducing an effective quadratic potential that accounts for the tendency of groups to be "pressed" towards their centre of mass by the action of the surrounding environment. This effect is similar to the one described by Moussaïd et al. (2010), whose microscopic model has 3 people groups

walking in an abreast formation at low densities and "closed" in a V formation at higher densities. One could wonder whether such an effect is present also in the data set we analysed in Zanlungo et al. (2014), and thus whether the V formations that we described in that work are due to the group internal dynamics (η) or due to the environmental effect ($C_{\rho_{\rm env}}$). Provided that, in order to settle this problem, the predictions of Moussaïd et al. (2010) and Zanlungo et al. (2014) should be tested in wider and less dense environments when such data sets will be available, we nevertheless believe that there are two reasons to prefer our model, at least to describe the behaviour of Japanese pedestrians in our data sets. The first reason is that we found V formations at densities much lower than those reported by Moussaïd et al. (2010) for the emergence of such a behaviour; and the second reason is that our internal dynamics mechanism is fundamental in explaining not only the group configurations, but also the group velocities.

References

Brščić, D., Kanda, T., Ikeda, T., Miyashita, T., 2013. Person tracking in large public spaces using 3-d range sensors. IEEE Transactions on Human Machine Systems 43 (6), 522–534.

Brščić, D., Zanlungo, F., Kanda, T., submitted. Density and velocity patterns during one year of pedestrian tracking. In: Pedestrian and Evacuation Dynamics 2014.

Costa, M., 2010. Interpersonal distances in group walking. Journal of Nonverbal Behavior 34 (1), 15–26.

Glas, D., Miyashita, T., Ishiguro, H., Hagita, N., 2009. Laser-based tracking of human position and orientation using parametric shape modeling. Advanced robotics 23 (4), 405–428.

Helbing, D., Molnar, P., 1995. Social force model for pedestrian dynamics. Phys. Rev. E 51 (5), 4282–4286.

Karamouzas, I., Overmars, M., 2010. Simulating the local behaviour of small pedestrian groups. In: Proceedings of the 17th ACM Symposium on Virtual Reality Software and Technology. ACM, pp. 183–190.

Kleinke, C. L., 1986. Gaze and eye contact: a research review. Psychological bulletin 100 (1), 78.

Knapp, M. L., 2012. Nonverbal communication in human interaction. Cengage Learning.

Köster, G., Seitz, M., Treml, F., Hartmann, D., Klein, W., 2011. On modelling the influence of group formations in a crowd. Contemporary Social Science 6 (3), 397–414.

Landau, L., Lifshitz, E., 1976. Mechanics (Course of Theoretical Physics, Vol 1). Butterworth Heinemann.

Landau, L., Lifshitz, E., 1980. Statistical Physics (Course of Theoretical Physics, Vol 5). Butterworth Heinemann.

Moussaïd, M., Perozo, N., Garnier, S., Helbing, D., Theraulaz, G., 2010. The walking behaviour of pedestrian social groups and its impact on crowd dynamics. PLoS One 5 (4), e10047.

Schultz, M., Rößger, L., Fricke, H., Schlag, B., 2014. Group dynamic behavior and psychometric profiles as substantial driver for pedestrian dynamics. In: Pedestrian and Evacuation Dynamics 2012. Vol. II. Springer, pp. 1097–1111.

Yücel, Z., Zanlungo, F., Ikeda, T., Miyashita, T., Hagita, N., 2013. Deciphering the crowd: Modeling and identification of pedestrian group motion. Sensors 13 (1), 875–897.

Zanlungo, F., Ikeda, T., Kanda, T., 2011. Social force model with explicit collision prediction. EPL (Europhysics Letters) 93 (6), 68005.

Zanlungo, F., Ikeda, T., Kanda, T., 2012. A microscopic social norm model to obtain realistic macroscopic velocity and density pedestrian distributions. PloS one 7 (12), e50720.

Zanlungo, F., Ikeda, T., Kanda, T., 2014. Potential for the dynamics of pedestrians in a socially interacting group. Phys. Rev. E 89 (1), 021811.

Zanlungo, F., Kanda, T., 2013. Do walking pedestrians stabily interact inside a large group? analysis of group and sub-group spatial structure. In: COGSCI13.

Zhang, Y., Pettré, J., Qin, X., Donikian, S., Peng, Q., 2011. A local behavior model for small pedestrian groups. In: Computer-Aided Design and Computer Graphics (CAD/Graphics), 2011 12th International Conference on. IEEE, pp. 275–281.